Optical and magnetic properties of $Zn_{1-x}Co_xO$ nanorod arrays fabricated by hydrothermal method

YALU ZUO, SHIHUI GE*, LI ZHANG, SHIMING YAN, XUEYUN ZHOU, YUHUA XIAO
Key Laboratory for Magnetism and Magnetic Materials of Ministry of Education, Lanzhou University, Lanzhou 730000, P.R. China

$Zn_{1-x}Co_xO$ (x = 0.1, 0.2) nanorods were prepared by hydrothermal method. The morphology of the nanorods was studied by field emission scanning electron microscopy. The results from x-ray diffraction and transmission microscopy indicated that the as-prepared nanorods were single-crystalline wurtzite structure. No metallic Co or other secondary phases were found. The vibrating sample magnetometer measurement demonstrate that $Zn_{0.8}Co_{0.2}O$ nanorods exhibit room temperature ferromagnetism (RTFM). The photoluminescence spectra implied that the nanorods exhibit strong orange emission.

(Received November 11, 2007; accepted November 26, 2007)

Keywords: $Zn_{1-x}Co_xO$ nanorods, Room temperature ferromagnetism, Photoluminescence

1. Introduction

ZnO nanomaterials have been extensively investigated for applications in luminescence, photocatalysts, gas sensors, solar cells and so on due to their specific electrical and optoelectronic properties [1, 2]. The properties of ZnO nanomaterials strongly depend on their dimensions and morphologies. Therefore, an investigation of ZnO nanostructures in highly oriented, aligned and ordered arrays is of critical importance for the development of novel devices [3, 4].

For the growth of highly aligned ZnO nanostructures, gas-phase deposition is one of the principal technologies. Although this approach can produce high-quality aligned ZnO nanostructures, it needs high temperature and metal catalyst particles to direct the aligned growth. Moreover, these techniques consume a large amount of energy and require equipment with rigorous experimental conditions. Therefore, such limitations inspired the research on solution-phase synthesis, which offers a great potential for a low-cost and large-scale fabrication [5-8]. The low-temperature solution methods (<110 ◦C) are particularly attractive because of their low energy requirements, safe and environmentally benign synthetic conditions. Recently, Greene *et al* [9] reported a two-step method for the growth of vertically aligned ZnO nanowires using a textured ZnO seed at 90 ^oC.

ZnO is a wide band gap semiconductor (3.37 eV) which has a large exciton binding energy (60 meV). Therefore, it is of great interest for practical applications in short wavelength photonic devices. In the photoluminescence (PL) spectra of ZnO, typically UV band-edge emission and one or more broad emission peaks in the visible range are observed. Among different visible emission peaks associated with defects, the green emission is the most common one [10]. However, ZnO nanostructures prepared by chemical methods typically exhibit yellow defect emission (centered at 580 nm) [11,12].

Diluted magnetic semiconductors (DMSs) have attracted considerable research interest in recent years due to their great potential applications in spintronic devices [13-19]. Some results have been achieved concerning the room-temperature ferromagnetism in Co-doped ZnO films and aggregated nanocrystals [20,21]. However, the synthesis and magnetic study of one dimensional Co-doped ZnO nanomaterials are still in a nascent stage [22, 23]. So, studies on fabrication in optical and magnetic properties of one dimensional Co-doped ZnO are interesting.

It is well known that the morphology of ZnO nanorods fabricated by hydrothermal methods is strongly dependent on the experimental conditions, such as solution concentration, growth temperature, and the substrate preparation. However, the effects of the dopant ions during hydrothermal growth have not been studied in detail. In this work, we studied the influence of the solution concentration and dopant on the morphology of fabricated ZnO nanorods. On the other hand, we investigated the the effect of dopant and annealing in forming gas (argon and hydrogen) on the optical properties of the nanorods.

2. Experimental

In this paper, high quality Co doped ZnO nanorods were synthesized by a simple hydrothermal route at low temperature (90 °C). The ZnO nanorods were grown by two steps. We first deposited ZnO seed layer on Si (100) substrates by the sol-gel method. Alcohol solutions of zinc acetate (0.5 M) and methenamine (0.5 M) were dipped in to Si (100) substrates. After subsequent spin coating, the substrates were annealed at 400 °C for one hour. At least two cycles were needed for the dense and uniform dispersion of ZnO nanoparticles on Si (100) substrates. The films were then put into a 50 ml sealed Teflon container which contained equimolar aqueous solution of zinc nitrate hexahydrate ($Zn(NO_3)_2{\cdot}6H_2O$) and hexamethylenetetramine ($C_6H_{12}N_4$). In detail, the different concentrations of 0.02 M, 0.05 M and 0.1 M of both $Zn(NO_3)_2{\cdot}6H_2O$ and $C_6H_{12}N_4$ in the resulting solution are acqiured. Then, the hydrothermal growth was carried out at 90 °C for 4 hours. Finally, the nanorod films were thoroughly washed with distilled water to eliminate residual salts, and dried in air at 60°C. In addition, we also fabricated $Zn_{1-x}Co_xO$ (x = 0.1, 0.2) nanorods by adding $Co(NO_3)_2{\cdot}6H_2O$ into aqueous solution.

X-ray diffraction (XRD), field emission scanning electron microscopy (FESEM) and transmission electron

microscopy (TEM) were used to characterize the structures and morphology of the nanorod films. Raman spectroscopy was also conducted as a supplementary tool to identify structural information. The optical and magnetic properties of the Co-doped ZnO nanorods were investigated by Photoluminescence (PL) spectrometry and vibrating sample magnetometer (VSM), respectively.

3. Result and discussion

Fig. 1a-c show the images of the undoped ZnO nanorods prepared with different concentration of 0.02 M, 0.05 M and 0.1 M of $Zn(NO_3)_2{\cdot}6H_2O$ and $C_6H_{12}N_4$, respectively. It can be observed that the ZnO nanorods were grown successfully on substrates with different solution concentration. The cross-section image of as-prepared nanorod arrays is shown in Fig.1b from which we note that all the nanorods grow vertically from the substrates and have a length of several hundreds nanometer (about 500 nm). Obviously, the concentration affects the obtained morphology. The nanorods are grown perpendicularly in a very high density over the whole substrate surface in Fig.1b (0.05 M) and Fig.1c (0.1 M) while the nanorods are somewhat disordered and in a low density in Fig.1a (0.02 M). Otherwise, the diameter of rods with 0.05 M is samller and more uniform than 0.1 M. The diameter of rods in Fig.1b is about 50-80nm and in Fig.1c is 80-200 nm. The small width and relatively large length results in the high aspect ratio, which is an important parameter in many applications.

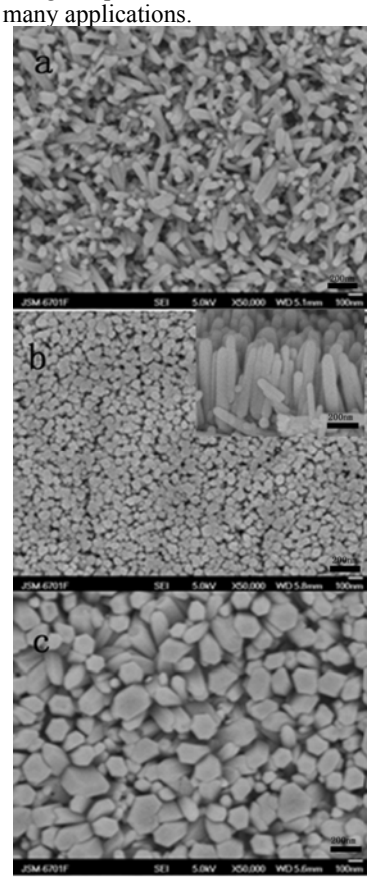

Fig.1. FESEM images of the ZnO nanorod films grown on Si (100) substrates with different solution concentration.

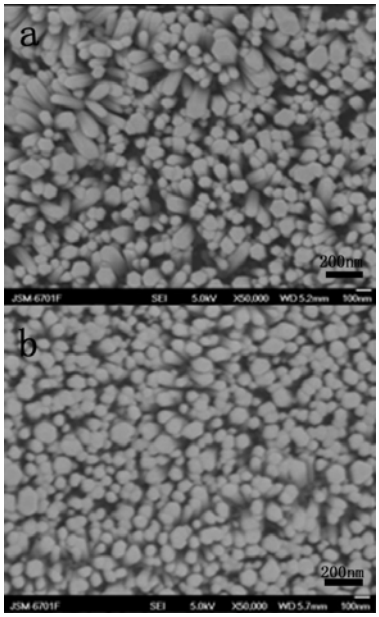

Fig. 2. FESEM images of the $Zn_{1-x}Co_xO$ nanorods with nominal Co concentration of x = 0.1 and x = 0.2.

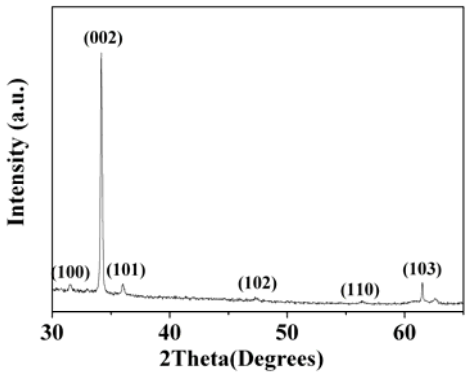

Fig.3. XRD pattern of $Zn_{0.8}Co_{0.2}O$ nanorod arrays.

From above result, the high density, uniform and well-orient ZnO nanorod arrays can be prepared with 0.05M. So we prepared $Zn_{1-x}Co_xO$ nanorods with this solution concentration. $Zn_{1-x}Co_xO$ nanorods prepared with nominal cobalt doping concentration of 10% and 20% are shown in Fig.2a and Fig.2b. It can be observed that with cobalt dopant, the nanorods are still uniform and perpendicular to the substrate but have lower density than pure ZnO nanorods.

The XRD patterns show that all nanorods have the wurtzite strucure of ZnO (hexagonal). Fig.3 shows the XRD pattern of the $Zn_{0.8}Co_{0.2}O$ nanorod arrays. All the diffraction peaks can be indexed to a ZnO wurtzite structure and no other impurity phase was found, which indicated the Co ion successfully occupied the lattice site. The strong relative intensity of the (002) lines reveals a texture effect of the arrays consistent with *c*-axis oriented nanorods [24].

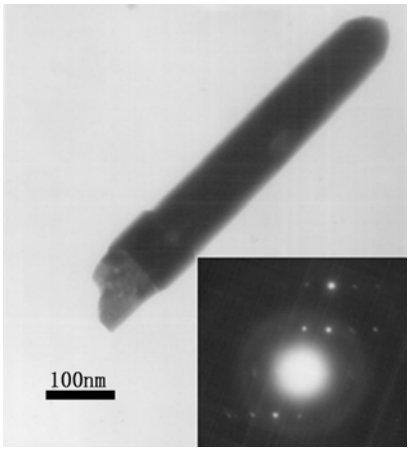

Fig.4. Typical TEM image of one single $Zn_{0.8}Co_{0.2}O$ nanorod (in inset is the corresponding SAED pattern).

The detailed structural characterization of the as-grown ZnO nanorod arrays was done by transmission electron microscopy (TEM). Fig.4 is a typical TEM image of one single $Zn_{0.8}Co_{0.2}O$ nanorod, its diameter is about 90 nm and length up to about 500nm. It is obviously that the nanorod has a clean and smooth surface and its bottom is a ZnO seed prepared in the first step. The corresponding selected area electron diffraction (SAED) pattern (inset of Fig.4) can be indexed to the [001] zone axis diffraction pattern of wurtzite structured ZnO [25], which is consistent with XRD results diffraction spots and rings denoting Co cluster cobalt oxide phases were found.

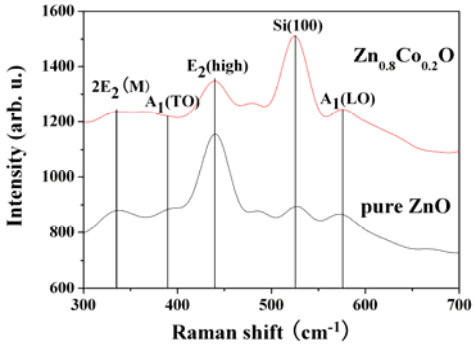

Fig.5. Raman spectra of pure ZnO and $Zn_{0.8}Co_{0.2}O$ nanorods.

Raman spectroscopy was conducted for ZnO nanorods to obtain the additional information for the film structure. Fig.5 shows the micro-Raman spectra of both pure ZnO and $Zn_{0.8}Co_{0.2}O$ nanorods at the range of 300–700 cm^{-1}. It is well known that the ZnO has eight sets of optical phonon modes $2A_1$, $2E_1$, $2E_2$ and $2B_1$. The basic frequencies of optical modes in ZnO are E_2 (low) = 101 cm^{-1}, E_2 (high) = 439 cm^{-1}, A_1 (TO) = 379 cm^{-1}, A_1 (LO) = 574 cm^{-1}, E_1 (TO) = 410 cm^{-1} and E_1 (LO) = 583 cm^{-1}. The second-order vibrations are at 208, 334 and 1050–1200 cm^{-1} arising from zone boundary phonons. The E_2 (high) is known to be the band characteristic of the wurtzite phase [26]. The position of the E_2 (high) mode of the ZnO is observed at 439 cm^{-1} for pure ZnO and $Zn_{0.8}Co_{0.2}O$ nanorods. It can be seen obviously that the peak at 439 cm^{-1} is lower by doping cobalt into ZnO due to the worse crystal structure. It can be considered as a evidence that Co dopant inhibits the growth of ZnO nanorods. Two more peaks have also been observed corresponding to A_1 (LO) and A_1 (TO) phonon mode at 575 and 389 cm^{-1} respectively. The observance of A_1 indicates that this mode is associated with the defects of O-vacancy, Zn-interstitial, or these complexes. No phonon peaks for E_1 (LO) and E_1 (TO) can be seen in the spectrum of ZnO nanorods. The peak located at 525 cm^{-1} is due to Si (100) substrate. The 332 cm^{-1} mode is attributed to the second order Raman process, which is twice that of the low-frequency E_2 phonon branch at the Brillouin-zone edge point (166 cm^{-1}) [27].

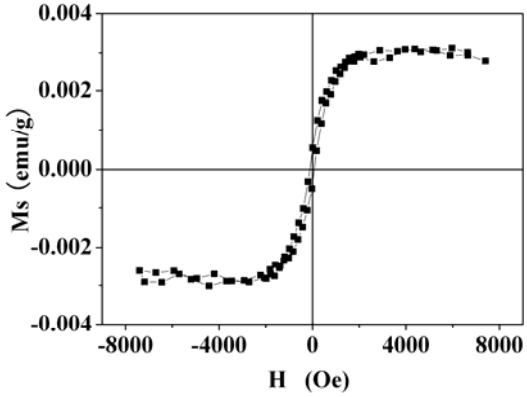

Fig.6. Room temperature hysteresis loop of $Zn_{0.8}Co_{0.2}O$ nanorods.

The magnetic properties of the Co doped nanorods were investigated by VSM. Fig.6 presents the M-H curves of the $ZnO_{0.8}Co_{0.2}O$ nanorods measured at 300K. The paramagnetic contribution from the sample holder has been subtracted from the data. There is a hysteresis loops with a coercivity of 100 Oe and a saturation magnetization of 0.003emu/g. As to the origin of ferromagnetic behavior observed in Co doped ZnO nanorods, there are a few of controversial explanations, one of which is the formation of some nanoscale Co-related secondary phase, such as metallic Co precipitation and Co oxides. In fact, Co oxides can be easily ruled out, since bulk CoO and Co_3O_4 is antiferromagnetism with Neel temperature of 293K and 33K respectively. Secondly, metallic Co is also a unlikely source of this ferromagnetism because the synthesis of Co-doped ZnO nanorods is performed in water as well as OH- which can prevent the formation of metallic Co nanoclusters to some extent. In addition, XRD and TEM results clearly show no metallic Co clusters and Co oxides in the nanorods. Thus ferromagnetism in the Co doped ZnO nanorods could be considered as a result of the exchange interaction between free delocalized carriers

(hole or electron from the valence band) and the localized *d* spins on the Co ions.

The PL spectra of ZnO typically exhibit UV emission and defect emission in the visible spectral range. Fig.7 presents the room temperature photoluminescence spectra (λex =325nm) for pure ZnO, $ZnO_{0.9}Co_{0.1}O$ and $ZnO_{0.8}Co_{0.2}O$ nanorods. The figure exhibits strong near band edge UV emission peaks centered at 391 nm, and noticeably, broad strong orange emissions centered at about 613 nm.

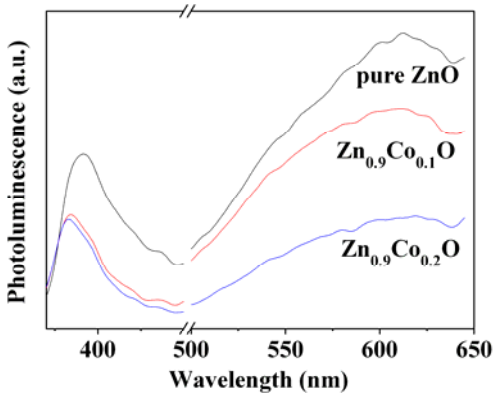

Fig. 7. PL spectra for pure ZnO, $Zn_{0.9}Co_{0.1}O$ and $Zn_{0.8}Co_{0.2}O$ nanorods recorded at room temperature (λ_{ex} =325nm).

It is known that the green emission results from the recombination of electrons with holes trapped in singly ionized oxygen vacancies and is commonly seen in ZnO materials synthesized under oxygen-deficient conditions [28]. The orange emission is less commonly reported and its origin, although not fully understood, seems to involve the presence of interstitial oxygen defects [29-32]. Compared with the pure ZnO, the orange emission peak intensities decreases in $ZnO_{0.9}Co_{0.1}O$ and $ZnO_{0.8}Co_{0.2}O$ nanorods because the dopants reduce the quantity of interstitial oxygen defects.

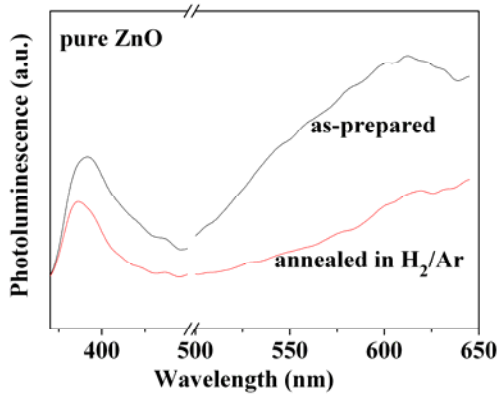

Fig. 8. PL spectra for as-prepared and annealing in forming gas of pure ZnO nanorods taken at room temperature (λ_{ex} = 325nm).

In order to verify whether the orange emission indeed originates from the interstitial oxygen defects, we performed investigation of the influence of annealing in forming gas of argon (90%) and hydrogen (10%) at 400°C. The obtained results of pure ZnO nanorods are shown in Fig.8. It can be observed that annealing in forming gas results in reduction of orange emission. The annealing for $ZnO_{0.9}Co_{0.1}O$ and $ZnO_{0.8}Co_{0.2}O$ nanorods obtained the same results.

Reduction of the visible emission by annealing in forming gas atmosphere is in agreement with previous reports [33-35]. It should be noted that hydrogen can have a dual role, it can assist the removal of excess oxygen or it can passivate the deep levels, which would result in reduced defect emission.

4. Conclusions

$Zn_{1-x}Co_xO$ nanorods were fabricated by a hydrothermal method from aqueous solutions of zinc nitrate hydrate, Cobalt nitrate hydrate, and hexamethylenetetramine. All of the as-prepared samples were single-crystalline wurtzite structure and no metallic Co or other secondary phases were found in the $Zn_{1-x}Co_xO$ nanorods. Otherwise, $Zn_{1-x}Co_xO$ nanorods exhibit room temperature ferromagnetism (RTFM). The PL spectra of pure ZnO and the $Zn_{1-x}Co_xO$ nanorods typically exhibit UV emission and orange emission. Moreover, it can be observed that annealing in forming gas results in reduction of orange emission.

Acknowledgment

This work is supported by National Natural Science Foundation of China (NO.50371034).

References

[1] D. C. Look, Mater. Sci. Eng.B-Solid-State Mater. Adv. Technol. **80**, 383 (2001).
[2] Z. R. Tian, J. A. Voigt, J. Liu, B. Mckenzie, M. J. Mcdermott, M. A. Rodriguez, H. Konishi, H. Xu, Nat. Mater. **2** 821 (2003).
[3] M. H. Huang, S. Mao, H. Feick, H. Yan, Y. Wu, H. Kind, E. Weber, R. Russo, P. Yang, Science. **292**, 1897 (2001).
[4] N. Beermann, L. Vayssieres, S.E. Lindquist, A.J. Hagfeldt, Electrochem. Soc. **147**, 2456 (2000).
[5] L. E. Greene, M. Law, J. Goldberger, F. Kim, J.C. Johnson, Y. Zhang, R.J. Saykally, P. Yang, Angew. Chem. Int. Ed. **42,** 3031 (2003).
[6] D. Li, Y.H. Leung, A. B. Djuris˘ ic′, Z. T. Liu, M. H. Xie, S. L. Shi, S. J. Xu, W. K. Chan, Appl. Phys. Lett. **85**, 1601 (2004).
[7] L. Vayssieres, Int. J. Mater. Product Technol. **18**, 330 (2003).

[8] M. Law, L. E. Greene, J. C. Johnson, R. Saykally, P. Yang, Nat. Mater. **4**, 455 (2005).
[9] L. E. Greene, M. Law, D. H. Tan, M. Montano, J. Goldberger, G. Somorjai, P. Yang, Nano. lett. **5**, 1231 (2005).
[10] A. B. Djurisˇ icʹ , W. C. H. Choy, V. A. L. Roy, Y. H. Leung, C. Y. Kwong, K. W. Cheah, T. K. Gundu Rao, W. K. Chan, H. F. Lui, C. Surya, Adv. Funct. Mater. **14**, 856 (2004).
[11] L. E. Greene, M. Law, J. Goldberger, F. Kim, J.C. Johnson, Y. Zhang, R. J. Saykally, P. Yang, Angew. Chem. Int. Ed. **42**, 3031 (2003).
[12] D. Li, Y.H. Leung, A. B. Djurisˇ icʹ , Z. T. Liu, M. H. Xie, S. L. Shi, S. J. Xu, W. K. Chan, Appl. Phys. Lett. **85**, 1601 (2004).
[13] S. D. Sarma, Nat. Mater. **2**, 292 (2003).
[14] S. J. Pearton, C. R. Abernathy, M. E. Overberg, G. T. Thaler, A. F. Hebard, Y. D. Park, F. Ren, J. Kim, L. A. Boatner, J. Appl. Phys. **1**, 93 (2003).
[15] H. Akinaga, H. Ohno, IEEE Trans Nanotechnol. **1**, 19 (2002).
[16] T. Dietl, Semicond. Sci. Technol. **17**, 377 (2002).
[17] I. Malajovich, J. J. Berry, N. Samarth, D. D. Awshalom, Nature. **411**, 770 (2001).
[18] H. Ohno, Science. **281**, 951 (1998).
[19] S. A. Wolf, D. D. Awschalom, R. A. Buhrman, J. M. Daughton, S. Von Molnar, M. L. Roukes, A.Y. Chtehelkanova, D. M. Treger, Science. **294**, 1488 (2001).
[20] Jae. Hyun. Kim, Hyojin. Kim , Dojin. Kim, Soon. Gil. Yoon and Woong. Kil. Choo, Solid State Communications. **131**, 677 (2004).
[21] Dana A. Schwartz, Nick S. Norberg, Quyen P. Nguyen, Jason M. Parker, Daniel R. Gamelin, J. Am. Chem. Soc. **125**, 13205 (2003).
[22] J. B. Cui, Q. Zeng, U. J. Gibson, J. Appl. Phys. **99**, 08M113 (2006).
[23] J. B. Cui, U. J. Gibson. Appl. Phys. Lett. **87**, 133108 (2005).
[24] Q Ahsanulhaq, A Umar, Y B Hahn, Nanotechnology. **18**, 115603 (2007)
[25] Min Guo, Peng Diaoc, Shengmin Cai, Applied Surface Science. **249**, 71 (2005).
[26] Sang-Hun Jeong, Jae-keun Kim and Byung-Teak Lee, J. Phys. D: Appl. Phys. **36**, 2017 (2003).
[27] Z. Q. Chen, A. Kawasuso, Y. Xu, H. Naramoto, X. L. Yuan, T. Sekiguchi, R. Suzuki, T. Ohdaira, J. Appl. Phys. **97**, 013528 (2005).
[28] J. C. Johnson, H. Yan, P. Yang, R. J. Saykally, J. Phys. Chem. B **107**, 8816 (2003).
[29] M. J. Zheng, L. D. Zhang, G. H. Li, W. Z. Shen, Chem. Phys. Lett. **363**, 123 (2002).
[30] T. Sekiguchi, S. Miyashita, K. Obara, T. Shishido, N. J. Sakagami, Cryst. Growth **214/215**, 72 (2000).
[31] X. L. Wu, G. G. Siu, C. L. Fu, H. C. Ong, Appl. Phys. Lett. **78**, 2285 (2001).
[32] S.A. Studenikin, N. Golego, M. J. Cocivera, Appl. Phys. 84 (1998) 2287.
[33] L. E. Greene, M. Law, J. Goldberger, F. Kim, J. C. Johnson, Y. Zhang, R. J. Saykally, P. Yang, Angew. Chem. Int. Ed. **42**, 3031 (2003).
[34] N. Ohashi, T. Ishigaki, N. Okada, T. Sekiguchi, I. Sakaguchi, H. Haneda, Appl. Phys. Lett. **80**, 2869 (2002).
[35] W. S. Shi, O. Agyeman, C. N. Xu, J. Appl. Phys. **91**, 5640 (2002).

*Corresponding author: gesh@ lzu.edu.cn; zuoyl04@lzu.cn